

# Chebyshev Pseudospectral Method for Nonlinear Stabilization using Control Contraction Metrics

Karen Leung and Ian R. Manchester

**Abstract**—Real-time implementation of the control contraction metric (CCM) method for nonlinear stabilization involves computation of a shortest path (a geodesic) between pairs of states. In this paper we propose the use of a direct numerical method, namely a Chebyshev pseudospectral method, to compute a geodesic. We investigate the influence of various parameters and tolerances and provide practical recommendations. We also compare the proposed method to a multiple-shooting algorithm (ACADO), and show that the proposed method is fast and accurate. An adaptive algorithm for finding a suitable degree and number of nodes is given. With an example nonlinear system, a controller is constructed using control contraction metrics and is compared against a linear controller and a controller calculated from nonlinear model predictive control, again using ACADO.

## I. INTRODUCTION

Control design for nonlinear dynamical systems continues to be a challenging problem. A common solution is to linearize the dynamics about a particular operating point or desired trajectory and apply linear design techniques. However, the system will in general only be locally stable and may become unstable far from the point of linearization. Another approach is to apply nonlinear model predictive control (NMPC), i.e. repeated on-line solution of a finite-horizon optimal control problem [1]. However, for nonlinear systems the associated optimization problems are generally non-convex due to the dynamic constraints, and can be difficult to solve in real time.

An elegant theory of necessary and sufficient conditions for stabilizability can be given in terms of control Lyapunov functions (CLF) [2]. However, the search for a CLF is generally non-convex, and constructive methods such as backstepping rely on the system having a particular triangular structure [3].

Contraction theory is an attractive alternate approach because it combines the simplicity of linear analysis with formal guarantees of global stability [4]. Recently, the concept of a control contraction metric (CCM) was introduced [5], [6]. A CCM is a Riemannian metric for which the associated distance between any pair of states can be made to decrease by control action. As such, existence of a CCM is a certificate of stabilizability of a nonlinear system. These conditions are necessary and sufficient for linear systems and feedback linearizable systems, and the search for a CCM can be made convex by a simple change of variables [6].

This work was supported by the Australian Research Council. The authors are with the Australian Centre for Field Robotics (ACFR), Department of Aerospace, Mechanical and Mechatronic Engineering, University of Sydney, NSW 2006, Australia {k.leung, i.manchester}@acfr.usyd.edu.au

Given a CCM, a state feedback controller can be constructed via an integration along a shortest path (a geodesic) between the system's current state and the target state [5], [6]. Therefore implementation of this scheme requires solving an optimization problem to find a geodesic. This on-line computation is analogous to NMPC, but is generally simpler due to the lack of dynamic constraints. Indeed, for many nonlinear systems a state-independent (a.k.a. "flat") CCM can be found, for which all geodesics are straight lines.

This paper is the first to consider computation of geodesics in the context of CCM and nonlinear stabilization, however geodesics naturally occur in many fields as they are the generalization to straight lines on curved spaces. A classical method of solution is to derive an explicit differential equation (the "geodesic equation") via the Euler-Lagrange equations, however for non-trivial metrics this will be difficult to solve [7]. Other methods that have been explored recently include the "Phase Flow Method" [8], fast marching [9], and graph cuts [10]. Although indirect methods would offer greater accuracy and confidence that first-order optimality conditions are met, disadvantages include small radii of convergence and the need to analytically derive the necessary conditions for each particular problem.

Direct methods are based on discretizing a shortest path or optimal control problem, and then solving the resulting nonlinear problem (NLP) using generic methods [11]. Depending on the method of discretization, this includes multiple shooting (e.g. [12]), direct collocation (e.g. [13]), and global pseudospectral (e.g. [14], [15], [16]).

In this paper, we propose a global pseudospectral approach using Chebyshev polynomials and nodes to solve the geodesic problem. An adaptive algorithm to find a suitable approximation of the geodesic is also given. Chebyshev polynomials are a good candidate for this pseudospectral method because they are numerically well conditioned and exhibit attractive convergence properties [17]. The authors of [14] and [15] explore the effectiveness of a Chebyshev pseudospectral method in solving a generic continuous Bolza optimal control problem (OCP). Similarly, [16] describes a unified framework based on Legendre-Gauss pseudospectral methods.

The structure of the paper is as follows: in Section II we define the problem and recall relevant facts about metrics, geodesics, and contraction analysis; in Section III we detail the proposed Chebyshev pseudospectral method; in Section IV we compare our method for computing geodesics to a multiple-shooting method implemented in the ACADO toolkit [18]; in Section V we compare the CCM control

method (incorporating the proposed geodesic computation) to LQR and NMPC; finally, we offer some brief conclusions.

## II. PRELIMINARIES AND PROBLEM FORMULATION

In this paper we consider nonlinear control affine systems, possibly time dependent, of the form:

$$\dot{x} = f(x, t) + B(x, t)u \quad (1)$$

where  $x(t) \in \mathbb{R}^n$  is the state and  $u(t) \in \mathbb{R}^m$  is the control, and  $t \in \mathbb{R}^+ := [0, \infty)$ . The function  $f : \mathbb{R}^n \times \mathbb{R}^+ \rightarrow \mathbb{R}^n$  is assumed to be smooth, and  $B : \mathbb{R}^n \times \mathbb{R}^+ \rightarrow \mathbb{R}^{n \times m}$  has columns  $b_i(x, t)$ ,  $i = 1, 2, \dots, m$ .

The objective is to design a state-feedback control policy that can globally exponentially stabilize *any* feasible trajectory of the system (1). A system is called *universally exponentially stabilizable* if this is possible [6].

### A. Metrics and Geodesics

A Riemannian metric equips a smooth manifold – which for this paper remains  $\mathbb{R}^n$  but can be more general – with an inner product on each tangent space, i.e.  $\delta_x^T M(x) \delta_x$  [19], [20]. This gives a local definition of length and orthogonality. Consider a smooth curve  $\gamma : [0, 1] \rightarrow \mathbb{R}^n$  with  $\frac{\partial \gamma}{\partial s} \neq 0 \forall s \in [0, 1]$ . Define  $e(s, \gamma) = \gamma_s^T(s) M(\gamma(s)) \gamma_s(s)$  where  $\gamma_s = \frac{\partial \gamma}{\partial s}$ . Then the length of the curve is defined as:

$$\ell(\gamma) = \int_0^1 \sqrt{e(s, \gamma)} ds \quad (2)$$

and this can be extended to piecewise-smooth curves by summing over smooth pieces.

A Riemannian metric defines a distance between points – The Riemannian distance – given by the infimum of lengths of curves joining the points. If the resulting metric space is complete, then the Hopf-Rinow theorem states that a minimizing path exists, which is a geodesic [20]. Geodesics are analogues of straight lines in curved space. A special property of a geodesic is that it has constant speed, i.e.  $e(s, \gamma)$  is independent of  $s \in [0, 1]$ . If  $\gamma$  is a geodesic, we have

$$\ell(\gamma)^2 = \int_0^1 e(s) ds =: E(\gamma),$$

where  $E(\gamma)$  is referred to as the energy of  $\gamma$ . So paths of minimum energy also have minimum length, and for numerical optimization the energy is preferred due to smoothness.

Classically, a minimal geodesic would be found by using the Euler-Lagrange equation to obtain necessary conditions in the form of an ordinary differential equation [7], but solving the associated two-point boundary value problem is generally non-trivial. Alternatively, the search for a geodesic can be expressed as a direct optimization over smooth paths:

$$\begin{aligned} \arg \min_{\gamma} \quad & \int_0^1 e(s) ds \\ \text{s.t.} \quad & \gamma(0) = x^*(t) \quad \gamma(1) = x(t). \end{aligned} \quad (3)$$

In this paper, we will use a Chebyshev pseudospectral method to discretize this problem, and then apply a quasi-Newton algorithm to the resulting nonlinear program.

### B. Control Contraction Metrics

Contraction analysis, as presented in [4], is based upon the study of the differential (linearized) dynamics of (1):

$$\dot{\delta}_x = A(x, u, t) \delta_x + B(x, t) \delta_u, \quad (4)$$

defined along each particular solution, where

$$A(x, u, t) := \frac{\partial f}{\partial x} + \sum_{i=1}^m \frac{\partial b_i}{\partial x} u_i.$$

Roughly speaking, if all solutions of a system are locally stable, then all solutions are globally stable [4]. This can be established by way of a contraction *metric*, i.e. a Riemannian metric  $M(x, t)$  for which the associated differential lengths  $\sqrt{\delta_x^T M(x, t) \delta_x}$  shrink exponentially with time.

A control contraction metric (CCM) is a Riemannian metric for which differential lengths can be *made* to shrink by control action. The main result of [6] is that if there exists a uniformly lower-bounded metric  $M(x, t)$  and satisfying

$$\delta_x' M B = 0 \implies \delta_x' (\dot{M} + A' M + M A + 2\lambda M) \delta_x < 0, \quad (5)$$

for all  $x, u, t$ , or – equivalently – a uniformly upper-bounded dual metric  $W(x, t)$  satisfying the pointwise LMI

$$B_{\perp}^T (-\dot{W} + A W + W A^T + 2\lambda W) B_{\perp} < 0, \quad (6)$$

for all  $x, u, t$ , then the system is universally exponentially stabilizable with rate  $\lambda$  by instantaneous feedback.

Finsler's theorem [21] states that (6) is equivalent to the existence of a scalar multiplier function  $\rho(x, t)$  satisfying

$$-\dot{W} + W A^T + A W - \rho B B^T < -2\lambda W \quad (7)$$

Note that (7) is jointly convex in  $W$  and  $\rho$ . If (1) has polynomial dynamics, then sum-of-squares programming [22] is a computationally tractable method to find  $W$  and  $\rho$ .

If a  $W(x, t)$  and  $\rho(x, t)$  satisfying (7) are found, then the control signal that stabilises the system to the desired trajectory  $x^*(t), u^*(t)$  is given by (8).

$$u(t) = u^*(t) - \frac{1}{2} \int_0^1 \rho(\gamma(s), t) B(t)^T W^{-1}(\gamma(s), t) \frac{\partial \gamma}{\partial s} ds \quad (8)$$

where  $\gamma(s)$  is a shortest path (geodesic) with respect to the metric  $M(x, t)$  connecting  $x^*(t)$  to  $x(t)$ .

In many cases, a “flat” CCM (independent of  $x$ ) can be found, for which every geodesic is a straight line. However, if a state-dependent metric is required then the CCM feedback controller requires on-line computation of a minimal geodesic associated with the CCM, i.e. a solution to Problem (3). It is precisely this computation that we address in the following sections.

## III. PSEUDOSPECTRAL METHOD

Since (3) is an infinite dimensional problem over all smooth curves, we need to discretize the problem to make it amenable to numerical solution. It is known that geodesics are smooth paths [19], so polynomials are a natural class of basis functions. Further, to carry out the integration, the interval  $[0, 1]$  needs to be discretized. In the pseudospectral

context, the discretization points are called collocation points or nodes. A good choice of polynomial basis, collocation points and integration scheme are essential for successful application.

In parametrising the geodesic, we will represent each coordinate  $\{x_1, x_2, x_3, \dots, x_n\}$  along the geodesic with (9).  $c_{ij}$  is the  $j$ th unknown coefficients of  $\gamma_i$  that need to be solved for,  $N$  is the maximum degree of the polynomial and  $\phi_j(s)$  is the  $j$ th degree polynomial basis function.

$$\gamma(s) = \begin{bmatrix} \gamma_1(s) \\ \gamma_2(s) \\ \vdots \\ \gamma_n(s) \end{bmatrix}, \quad \gamma_i(s) = \sum_{j=0}^N c_{ij} \phi_j(s). \quad (9)$$

Chebyshev polynomials are chosen because they can be easily represented through a recursive formula and can be made to be orthogonal on the  $[0, 1]$  interval after using an affine transformation. Further, they exhibit attractive convergence properties and have the smallest maximum pointwise error compared to any other polynomials. Thus Chebyshev polynomials are often the default choice [17]. In addition, the Chebyshev-Gauss-Lobatto (CGL) nodes are used because they are given by a simple analytic formula and are more numerically well conditioned than equally space nodes [17]. Further, the Clenshaw-Curtis quadrature (CCQ) scheme that is derived from using CGL nodes has weights which are also given by a simple analytic formula [15], [23].

#### A. Discretisation of the Problem

In describing the basis functions, define  $T_k(s)$  as the  $k^{\text{th}}$  degree Chebyshev of the first kind polynomial basis function. Then the derivative can be denoted by  $DT_k(s) := \frac{dT_k}{ds}$ . Since the coefficients appear linearly, the differentiation needed to compute the gradient function can be done analytically. Each of the coordinates  $\gamma_i$  along the geodesic will have its associated differential lengths  $\gamma_{s_i}$ . It will have the form

$$\gamma_i(\mathbf{c}; s) = \sum_{j=0}^N c_{ij} T_j(s), \quad \frac{\partial \gamma_i}{\partial s} := \gamma_{s_i}(\mathbf{c}; s) = \sum_{j=0}^N c_{ij} DT_j(s). \quad (10)$$

where  $\mathbf{c}$  is the decision vector containing all the coefficients:

$$\mathbf{c} = (c_{10}, c_{11}, \dots, c_{1N}, c_{20}, c_{21}, \dots, c_{2N}, \dots, c_{n0}, c_{n1}, \dots, c_{nN}).$$

Recall  $N$  is the degree of the polynomial and  $n$  is the dimension of the state space in (1). So the size of the problem will be  $(N+1) \times n$ .

Integration of a function along a curve approximated by a weighted sum of function evaluation at a finite set of nodes. The CGL nodes  $\{s_k\}$  are defined as follows:

$$s_k = \cos\left(\frac{\pi k}{K}\right), \quad k = 0, 1, \dots, K. \quad (11)$$

The CCQ quadrature scheme is a weighted sum based on an expansion of the integrand in terms of Chebyshev polynomials:

$$\int_0^1 p(s) ds = \sum_{k=0}^K p(s_k) w_k, \quad p(s) \in \mathcal{P}_N \quad (12)$$

Here  $\mathcal{P}_N$  is the space of polynomials of degree  $N \leq K$ . The weighting given to each node is given by

$$w_0 = w_K = \frac{1}{\tilde{K}}, \quad k = 1, \dots, \frac{\tilde{K}}{2} \quad (13)$$

$$w_k = w_{N-k} = \frac{2}{\tilde{K}} \sum_{j=0}^{\tilde{K}/2''} \frac{1}{1-4j^2} \cos \frac{2\pi jk}{\tilde{K}}$$

where  $\hat{K} = K^2 - 1$  and  $\tilde{K} = K$  if  $K$  is even or  $\hat{K} = K^2$  and  $\tilde{K} = K - 1$  if  $K$  is odd. The double prime means the first and last terms are halved.

The CCQ integration scheme is exact for  $N = K$  if  $p(t) \in \mathcal{P}_N$ . However, in general  $M(x, t)$  will not be polynomial, since it is obtained by inverting  $W(x, t)$ . As such,  $K > N$  is needed for a feasible solution and an exploration for a sufficiently large  $K$  is given in Section III-C.

We can now substitute (10) into our optimization problem (3). The constraints now have a nice form since

$$T_k(0) = \begin{cases} 1 & \text{if } \frac{k}{2} \text{ even} \\ 0 & \text{if } k \text{ odd} \\ -1 & \text{if } \frac{k}{2} \text{ odd} \end{cases}, \quad T_k(1) = 1 \quad \forall k \in \mathbb{N}.$$

Let  $P = [T_0(0), T_1(0), T_2(0), \dots, T_N(0)]$  be a row vector and  $\mathbf{0}$  a row vector of zeros of the same length and likewise  $\mathbf{1}$  a row vector of ones. Then the linear constraint becomes  $\mathcal{C} = A\mathbf{c} - b$  where  $A$  and  $b$  is give below.

$$\mathcal{C}(\mathbf{c}) := \underbrace{\begin{bmatrix} P & \mathbf{0} & \dots & \mathbf{0} \\ \mathbf{0} & P & \dots & \mathbf{0} \\ \vdots & \vdots & \ddots & \vdots \\ \mathbf{0} & \mathbf{0} & \mathbf{0} & P \\ \mathbf{1} & \mathbf{0} & \dots & \mathbf{0} \\ \mathbf{0} & \mathbf{1} & \dots & \mathbf{0} \\ \vdots & \vdots & \ddots & \vdots \\ \mathbf{0} & \mathbf{0} & \mathbf{0} & \mathbf{1} \end{bmatrix}}_A \mathbf{c} - \underbrace{\begin{bmatrix} x^*(t) \\ x(t) \end{bmatrix}}_b = \mathbf{0} \quad (14)$$

As such, the optimization problem in (3) can be expressed as (15). This is a smooth nonlinear optimization problem with linear constraints.

$$\begin{aligned} \underset{\mathbf{c}}{\text{argmin}} \quad & \sum_{k=0}^K \gamma_s(\mathbf{c}, s_k)^T M(\gamma(\mathbf{c}, s_k), t) \gamma_s(\mathbf{c}, s_k) w_k =: E(\mathbf{c}) \\ \text{s.t.} \quad & \mathcal{C}(\mathbf{c}) = \mathbf{0} \end{aligned} \quad (15)$$

#### B. Quasi-Newton Optimization

After discretization, the problem is a finite-dimensional NLP with linear constraints. Since gradients are relatively straightforward to compute, but Hessians less so, we employ the BFGS quasi-Newton strategy, which recursively approximates the Hessian using successive gradient evaluations and a secant condition [24]. To ensure first-order optimality conditions are met, the KKT matrix given by (16) is solved at each iteration of the optimization algorithm.

$$\begin{bmatrix} H & A^T \\ A & 0 \end{bmatrix} \begin{bmatrix} -p \\ \lambda \end{bmatrix} = \begin{bmatrix} g \\ \mathcal{C} \end{bmatrix} \quad (16)$$

In Algorithm 1,  $E$  is the objective function,  $g$  is the gradient,  $H$  is the approximate Hessian,  $p$  is the step direction and  $\alpha$  is the step size determined by a backtracking line search (Line 11).

In calculating  $g$  (Line 5, 16), we use the relation  $\dot{M} = -M\dot{W}M$  (the dot represents a differentiation in any argument). Thus each component of  $g$  is given by (17).

$$\frac{\partial f}{\partial c_{ij}} = \sum_{k=1}^K 2\gamma_s^T M D T_j d s_k - \gamma_s^T M \frac{\partial W}{\partial x_i} M \gamma_s T_j d s_k \Big|_{\mathbf{c}, s_k} \quad (17)$$

To update the Hessian (L17), the BFGS formulae [24] is used and is given by (18). Here,  $y = g - g_0$  and  $H_p$  is the Hessian from the previous iteration. The identity matrix is sufficient as an initial guess of the Hessian (Line 6).

$$H_{p+1} = H_p - \frac{H_p s s^T H_p}{s^T H_p s} + \frac{y y^T}{y^T s} \quad (18)$$

The inputs into the algorithm are separated into the settings of the BFGS quasi-Newton (L1) and the problem specifications (Line 2). The settings consist of the tolerance ( $\beta$ ) to terminate the optimization algorithm (Line 7), the initial step size of the line search  $\alpha_0$  (Line 9), the termination condition for the line search  $\bar{c}$  (Line 11) and the rescaling factor  $\tau$  (Line 12) for the backtracking line search. The problem specification refers to the information that describes the contraction metric and the representation of the solution. It consists of the metric  $W$ , the degree of the Chebyshev polynomial  $N$ , the number of nodes  $K$ ,  $x(t)$  and  $x^*(t)$ . The linear constraint  $A\mathbf{c} - b = 0$  is given by (14) and an initial guess for  $\mathbf{c}_0$  is simply a straight line (Line 5)

$$\mathbf{c}_0 = (x_1, (x_1^* - x_1), 0, \dots, x_2, (x_2^* - x_2), 0, \dots, x_n, (x_n^* - x_n), 0, \dots). \quad (19)$$

For  $x(t)$  and  $x^*(t)$  close, the initial guess will be a good approximation since geodesics are locally straight lines.

### C. Adaptive Degree Selection

In this section, we propose an algorithm for selecting the minimal degree  $N$  to obtain a geodesic with sufficient accuracy. Recall that a geodesic has constant speed along the path. Since this constraint is not imposed during the optimization, the deviation of  $e(s, \gamma)$  from the constant squared speed can be used as an independent validation that the solution found is a geodesic. The value for the energy  $E^*$  obtained from the optimization is used to formulate a measure of mismatch from constant speed:

$$\mathcal{E} = \int_0^1 \frac{|e(s) - E^*|}{E^*} ds \quad (20)$$

Once again, the CCQ rule and CGL nodes are used to carry out the integration. For a true geodesic  $\mathcal{E} = 0$ .

Given the facts: (i) set of all polynomials on  $[0, 1]$  spans the set of smooth curves, (ii) by increasing the maximum degree we enlarge the set of curves that can be represented, and (iii) the curve of minimal energy has constant speed, we propose to simply increase the degree until  $\mathcal{E}$  is reduced below a certain threshold, see Algorithm 2.

---

### Algorithm 1 BFGS

---

- 1: Input settings for the problem ( $\beta, \alpha_0, \bar{c}, \tau$ ).
  - 2: Input solution specifications ( $W, N, K, x, x^*$ ).
  - 3: Evaluate polynomials using (10) and weights using (13) at the node points which are computed using (11).
  - 4: Construct  $A$  and  $b$  constraint matrix using (14).
  - 5: Initialise  $\mathbf{c} = \mathbf{c}_0$  using (19) and  $g_0 = g|_{\mathbf{c}_0}$  using (17) and  $E_0 = E|_{\mathbf{c}_0}$  using (15).
  - 6: Initialise  $H_0 = I$
  - 7: **while**  $\|\alpha p\| > \beta$  **do**
  - 8:   Compute  $p$  by solving the KKT conditions using (16)
  - 9:    $\alpha \leftarrow \alpha_0$
  - 10:    $E = E(\mathbf{c}_0 + \alpha p)$
  - 11:   **while**  $E_0 - E < \alpha g p \bar{c}$  **do** ▷ Line Search
  - 12:      $\alpha \leftarrow \alpha \tau$
  - 13:      $E = E(\mathbf{c}_0 + \alpha p)$
  - 14:   **end while**
  - 15:    $s = \alpha p$
  - 16:   Update  $\mathbf{c} \leftarrow \mathbf{c}_0 + s$ ,  $E \leftarrow E(\mathbf{c})$ ,  $g \leftarrow g(\mathbf{c})$
  - 17:   Update  $H$  using BFGS formula given by 18
  - 18:    $\mathbf{c}_0 \leftarrow \mathbf{c}$ ,  $g_0 \leftarrow g$ ,  $H_0 \leftarrow H$ ,  $E_0 \leftarrow E$ .
  - 19: **end while**
- 

---

### Algorithm 2 Adaptive selection for $N$

---

- 1: Inputs for optimization
  - 2: **for**  $N = N_{min} : N_{max}$  **do**
  - 3:   BFGS optimization
  - 4:   **if**  $\mathcal{E} < \varepsilon$  **then**
  - 5:     break
  - 6:   **end if**
  - 7: **end for**
- 

It is not only  $N$  that needs to be chosen, but also the tolerance  $\beta$  and number of nodes  $K$ . However, it was found that these parameters have comparatively little effect and can be fixed in advance. An analysis on the optimization component showed that increasing  $K$  is more computationally expensive than increasing  $\beta$ . As such, to ensure that  $\|\Delta e\|$  is always very small, we can make  $\beta = 10^{-10}$  without compromising on computation time too much. Since  $e(s)$  is not guaranteed to be polynomial,  $K = N$  would not give reliable results when using CCQ. Instead, we consider values for  $K$  in the form of  $K = N + a$ . This offers smallest possible  $K$  values. A high  $K$  value of  $K = N + 100$  was used as a benchmark comparison, and this was compared with other values for  $a$ . It was found that for  $a = 3$ , there was not much difference between the benchmark in terms of accuracy and computation costs. Through experimentation of different  $\varepsilon$  values in Algorithm 2, it was found  $\varepsilon = 10^{-5}$  is a suitable.

During real-time operation, the input for Algorithm 2 consists of  $W$ ,  $x(t)$  and  $x^*(t)$ , and a minimal  $N$  and the associated coefficients for the geodesic are the outputs.  $N = 1$  is a natural lower bound for  $N$  to test.

#### IV. ILLUSTRATIVE EXAMPLE

To illustrate, the following system was used to obtain a control contraction metric and to calculate a geodesic from it. The system (21) was investigated in [6] and [25]. This is an interesting system to analyze because local controllers fail globally and it is stiff and highly unstable. In [25], the problem of uniting a locally optimal and globally stabilising controller is explored. In the CCM framework, this problem can be easily formulated because the search for  $W$  is over a convex set.

$$\begin{bmatrix} \dot{x}_1 \\ \dot{x}_2 \\ \dot{x}_3 \end{bmatrix} = \begin{bmatrix} -x_1 + x_3 \\ x_1^2 - x_2 - 2x_1x_3 + x_3 \\ -x_2 \end{bmatrix} + \begin{bmatrix} 0 \\ 0 \\ 1 \end{bmatrix} u \quad (21)$$

Sum-of-squares programming was carried out on Yalmip [26] and the semidefinite programming solver MOSEK. The metric is enforced to match LQR locally about zero [6]. Here,  $W(0, t) = P^{-1}$  where  $P$  is the solution to the algebraic Riccati equation

$$A(0)'P + PA(0) - PBR^{-1}B'P + Q = 0$$

with  $Q = I$  and  $R = I$ . A control contraction metric with  $\lambda = 0.5$  and a lower limit of  $\alpha_1 = 1 \times 10^{-4}$  was found to be

$$W(x, t) = W_0 + W_1x_1 + W_2x_1^2$$

where

$$W_0 = \begin{bmatrix} 2.286 & 0.143 & -0.429 \\ 0.143 & 1.571 & 0.286 \\ -0.429 & 0.286 & 1.143 \end{bmatrix}$$

$$W_1 = \begin{bmatrix} 0 & -4.571 & 0 \\ -4.571 & -0.572 & 0.857 \\ 0 & 0.857 & 0 \end{bmatrix} \quad W_2 = \begin{bmatrix} 0 & 0 & 0 \\ 0 & 9.143 & 0 \\ 0 & 0 & 0 \end{bmatrix}$$

and  $\rho(x, t) = 2 + 1.264x_1 + 8.157x_1^2$ . This is a relatively simple nonlinear metric because it only depends on the first state and it is only quadratic in the  $(2, 2)$  entry. It was shown in [6] that metrics of this form are complete, and thus a minimal geodesic exists between every pair of points.

The proposed Chebyshev pseudospectral method is one way of finding a geodesic. Another way is to reformulate the geodesic problem as an OCP with differential constraints. The OCP can then be solved using an optimization software such as ACADO.

##### A. Finding a Geodesic: Chebyshev Pseudospectral Method

The CCM for (21) is analyzed and solutions to the optimization algorithm and a suitable degree were found for various end points using Algorithm 2. Figure 1 shows that there is little variation in computation time as  $\beta$  increases, but the cost of increasing  $K$  is significant. The  $N = K$  case is not considered because it was not reliable since  $e(s)$  is not polynomial. It can be seen in Figure 2 that for  $K = N + 3$ ,  $\mathcal{E}$  closely follows the benchmark given by when  $K = N + 100$ . For  $K = N + 1, N + 2$  there is a larger discrepancy for smaller  $N$ , but they all overlap at larger  $N$ . However,  $N$  needs to be minimal since this reduces the size of the problem and

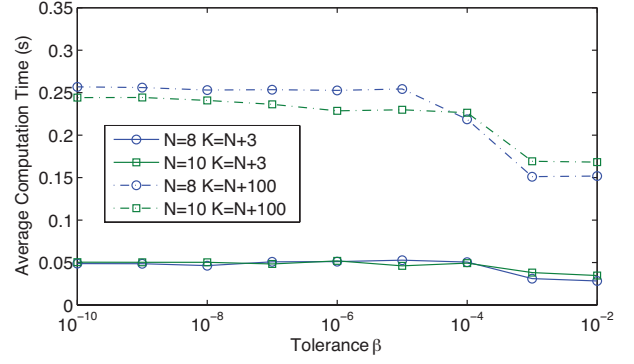


Fig. 1. Computation time using a Chebyshev pseudospectral method as  $\beta$ ,  $K$  and  $N$  varies. Geodesic from  $[0, 0, 0]^T$  to  $[9, 9, 9]^T$ .

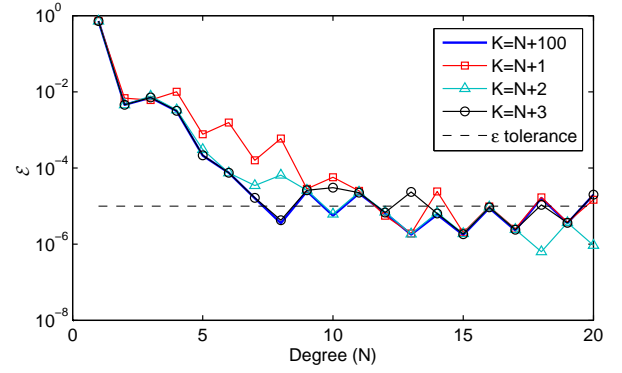


Fig. 2. Using a Chebyshev pseudospectral method,  $\mathcal{E}$  as  $N$  varies for different values of  $K$ . Geodesic from  $[0, 0, 0]^T$  to  $[9, 9, 9]^T$ .

hence computation time. The computation time is the time taken for Algorithm 1 to converge. From Figure 3, the cost of increasing  $N$  is larger than the cost of increasing  $K$  by a few nodes. Using Algorithm 2, solutions were found for geodesics joining  $[0, 0, 0]^T$  to different points, shown in Table I. The computation times given represent the time taken to iterate through different  $N$ 's until  $\mathcal{E}$  fell below the tolerance. The results were obtained on a computer running a 3.60GHz Intel i7-4790. Figures 4 and 5 show the variations in energy along the geodesic with different end points at a close up view. While Figures 6 and 7 compare the energy along the geodesic between the chosen  $N$  and using lower degrees and it can be seen than for the chosen  $N$ , the deviations in energy are very small, implying that the polynomial basis chosen is sufficiently large to approximate the geodesic accurately. In

TABLE I  
USING ALGORITHM 2 TO FIND GEODESICS WITH  $x^*(t) = 0$ .

$x(t)$	$N^*$	$\mathcal{E}_N$	Avg. comp. time
$[0.1, 0.1, 0.1]^T$	2	$2.719 \times 10^{-8}$	0.0579
$[1, 1, 1]^T$	3	$5.684 \times 10^{-6}$	0.0763
$[3, 3, 3]^T$	4	$6.214 \times 10^{-7}$	0.113
$[5, 5, 5]^T$	5	$1.421 \times 10^{-6}$	0.178
$[7, 7, 7]^T$	5	$8.160 \times 10^{-6}$	0.179
$[9, 9, 9]^T$	8	$4.258 \times 10^{-6}$	0.379

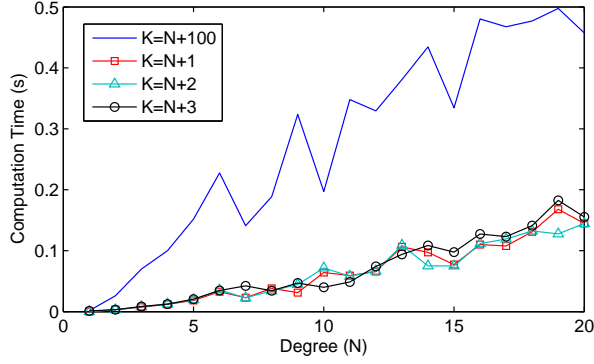


Fig. 3. Computation time as  $K$  and  $N$  varies using a Chebyshev pseudospectral method. Geodesic from  $[0,0,0]^T$  to  $[9,9,9]^T$ .

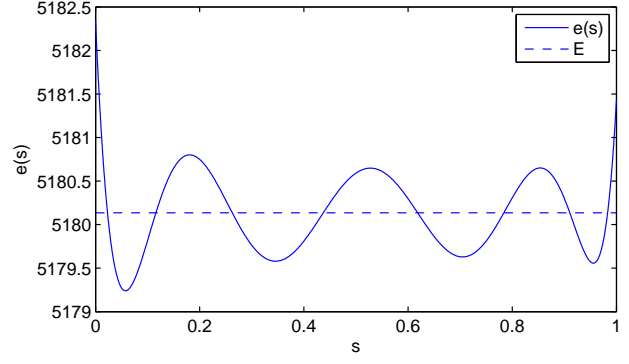


Fig. 5. Energy along the geodesic using a Chebyshev pseudospectral method.  $N = 8$ . Geodesic from  $[0,0,0]^T$  to  $[9,9,9]^T$ .

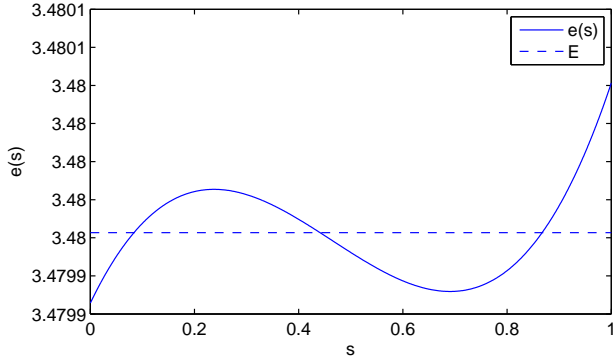


Fig. 4. Energy along the geodesic using a Chebyshev pseudospectral method.  $N = 3$ . Geodesic from  $[0,0,0]^T$  to  $[1,1,1]^T$ .

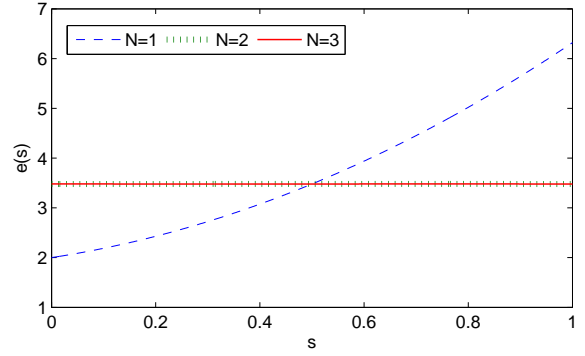


Fig. 6. Comparison of energy along the geodesic with different  $N$  using a Chebyshev pseudospectral method. Geodesic from  $[0,0,0]^T$  to  $[1,1,1]^T$ .

Figure 6,  $N = 2$  and  $N = 3$  look almost identical because  $\mathcal{E}$  are both very small ( $\mathcal{E} = 1.242 \times 10^{-5}$  and  $5.684 \times 10^{-6}$  respectively) but  $N = 3$  was when  $\mathcal{E}$  fell below the tolerance first.

### B. Finding a Geodesic: ACADO

The geodesic problem can also be expressed as a simple OCP by replacing  $s$  with time and introducing trivial dynamical constraints:

$$\begin{bmatrix} \dot{x}_1 \\ \dot{x}_2 \\ \dot{x}_3 \end{bmatrix} = \begin{bmatrix} u_1 \\ u_2 \\ u_3 \end{bmatrix}, \quad J = \int_0^1 u^T M(x) u dt$$

This OCP can be solved using ACADO which multiple shooting: it approximates  $u$  as piecewise constant, and  $\gamma$  as piecewise linear. The default KKT tolerance of  $10^{-6}$  was used.

The computation time to find the geodesic using ACADO was significantly greater than the Chebyshev pseudospectral method as seen in Figure 8. Even with 100 segments, the  $\mathcal{E}$  value for a  $x(t) = [9,9,9]^T$  and  $x(t) = [1,1,1]^T$  is still significantly greater than the results from using the Chebyshev pseudospectral method. The changes in  $\mathcal{E}$  as the number of segments increase is presented in Figure 9. The trapezoidal rule was used to carry out the integration. Increasing the number of segments to help improve accuracy

would be impractical in terms of computation time according to the trend shown in Figure 8.

As such, compared to the multiple shooting method in ACADO, the Chebyshev pseudospectral method is significantly faster and more accurate with less nodes.

## V. CONTROLLER DESIGN

In this section, we compare CCM with the proposed pseudospectral scheme to two popular methods for control: LQR and NMPC. Once again, the nonlinear system was given in (21) and the computation of the CCM is as above. A CCM controller is constructed at each time step by solving the geodesic problem using the proposed Chebyshev pseudospectral method and integrating the differential control along this path. This controller is compared against a linear controller obtained by computing the LQR for the system linearized at the origin. A multiple-shooting NMPC regime was implemented ACADO. Simulations were computed using a fourth order Runge-Kutta scheme, and ACADO was applied with a 4/5th order Runge-Kutta scheme.

### A. Starting Close to the Origin

We first consider the case when the states start at  $x(0) = [1,1,1]^T$  and  $x^*(t) = [0,0,0]^T$ . Figure 10 shows trajectory of the states from applying the CCM, LQR and NMPC controller. As expected, they are almost indistinguishable

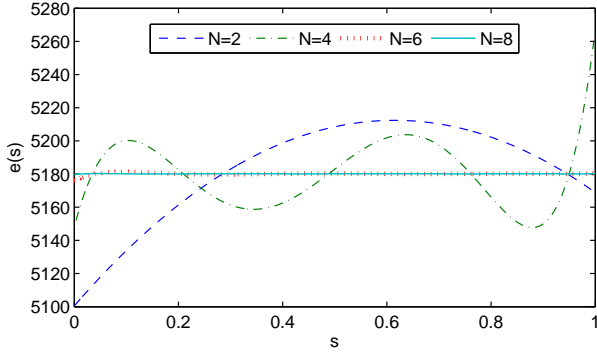


Fig. 7. Comparison of energy along the geodesic with different  $N$  using a Chebyshev pseudospectral method. Geodesic from  $[0, 0, 0]^T$  to  $[9, 9, 9]^T$ .

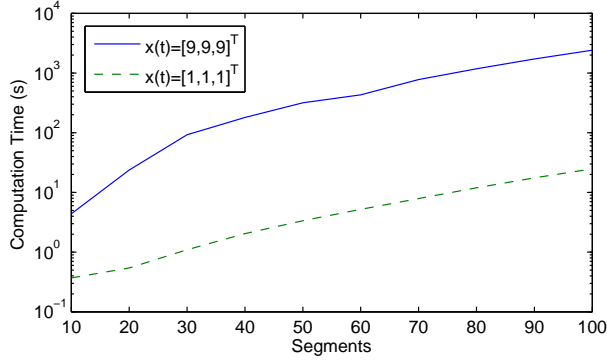


Fig. 8. Average computation using ACADO to find a geodesic with different  $x(t)$  and  $x^*(t) = [0, 0, 0]^T$  as the number of segments increases. Compare with Figure 3.

since they are all locally optimal in an LQ sense. Since the start and end points of the geodesic are close, a lower degree polynomial was used. As the distance becomes even smaller, the geodesic is close to a straight line and so the feedback controller (8) essentially becomes a simple linear feedback, similar to LQR. Obviously, LQR had the fastest computation time since it only uses very simple calculations. The time to compute a single control signal for each method is given in Figure 11. CCM was significantly faster than NMPC. A time step of 0.2 seconds was used.

Starting from a larger initial condition:  $x(0) = [9, 9, 9]^T$ , LQR did not stabilize the system whereas CCM was still successful, as seen in Figure 12. Since the system is very stiff, a very small time step was needed ( $< 0.01s$ ). ACADO was not able to compute a solution from this initial condition, which we believe is due to the stiffness of the ODE: the slow dynamics require a long time horizon, and the fast dynamics require a short sampling time, leading to a very large number of required nodes.

The computation time required to compute each control input for CCM is depicted in Figure 13. As can be seen, as the system state approaches the origin the required computation time decreases.

To summarise: for this system, LQR was effective only for regions local to the point of linearization, while multiple

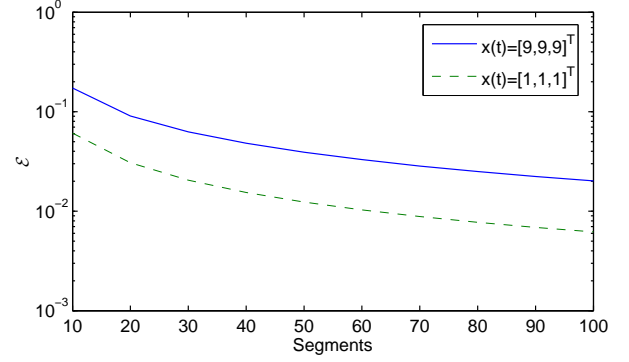


Fig. 9.  $\mathcal{E}$  of a geodesic found using ACADO with different  $x(t)$  and  $x^*(t) = [0, 0, 0]^T$  as the number of segments increases.

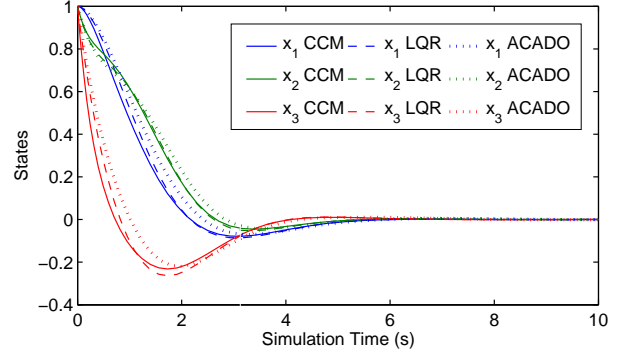


Fig. 10. States starting at  $[1, 1, 1]^T$  with different controller design.

shooting NMPC using ACADO required many discretization points and did not succeed for large initial conditions. CCM gave stabilising results with starting points far from the origin, and the computation time was significantly faster than NMPC.

## VI. CONCLUSIONS

In this paper we examined the on-line computation required for nonlinear stabilization using the control contraction metric approach. The Chebyshev pseudospectral method was found to be a rapid and accurate way to approximate the required minimal geodesic. It has benefits over multiple shooting methods in that it requires significantly less nodes without sacrificing accuracy. The CCM method was used to compute a stabilising controller for an example system and was compared against LQR and NMPC using ACADO's multiple shooting algorithm. CCM was able to stabilise the system beyond LQR's region of stability and it was found a multiple shooting method was very difficult to implement on a stiff system. We conclude that the CCM/Chebyshev-pseudospectral method presents a viable alternative for certain difficult nonlinear stabilization problems, and in some sense represents a middle ground between the simplicity of LQR and the global performance of NMPC.

## REFERENCES

- [1] F. Allgöwer and A. Zheng, *Nonlinear model predictive control*. Birkhauser, 2012, vol. 26.



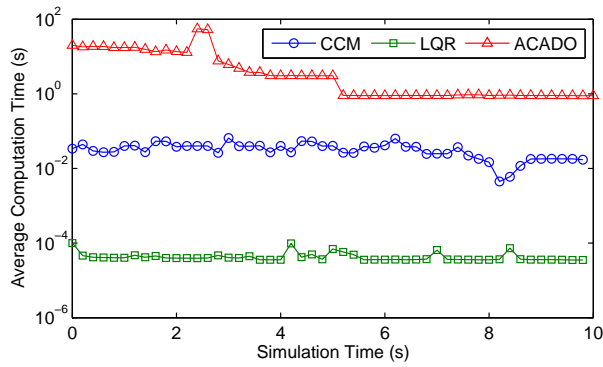


Fig. 11. Comparison of computation time to compute control signal with states starting close to the origin.

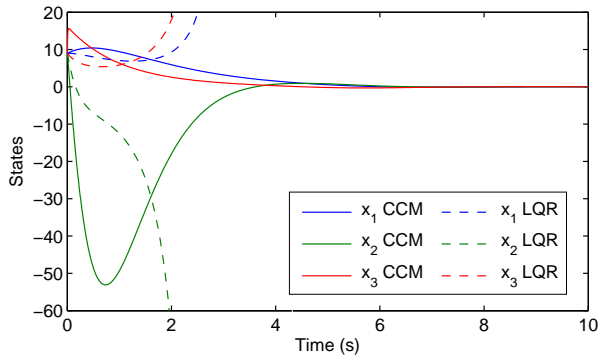


Fig. 12. States starting at  $[9, 9, 9]^T$  with different controller design. Could not obtain feasible solution with ACADO.

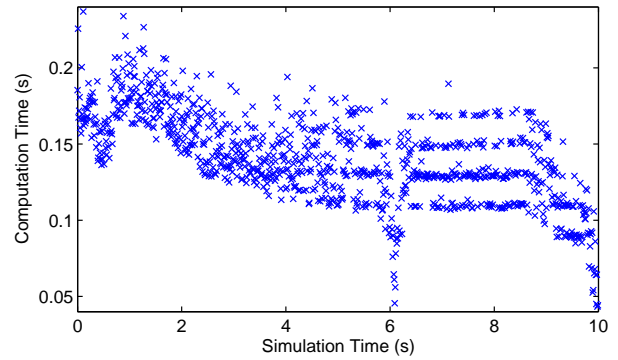


Fig. 13. Computation time to compute a CCM control signal starting at  $[9, 9, 9]^T$ .

- [2] E. D. Sontag, "A universal construction of Artstein's theorem on nonlinear stabilization," *Systems & Control Letters*, vol. 13, no. 2, pp. 117–123, Aug. 1989.
- [3] M. Krstic, I. Kanellakopoulos, and P. Kokotovic, *Nonlinear and adaptive control design*. Wiley, 1995, vol. 222.
- [4] W. Lohmiller and J.-J. E. Slotine, "On Contraction Analysis for Nonlinear Systems," *Automatica*, vol. 34, no. 6, pp. 683–696, June 1998.
- [5] I. R. Manchester and J.-J. E. Slotine, "Control Contraction Metrics and Universal Stabilizability," in *Proceedings of the IFAC World Congress*, Cape Town, South Africa, 2014.
- [6] —, "Control Contraction Metrics: Convex and Intrinsic Criteria for Nonlinear Feedback Design," *arXiv:1503.03144*, Mar. 2015.
- [7] V. I. Arnold, *Mathematical methods of classical mechanics*. Springer Science & Business Media, 1989, vol. 60.
- [8] L. Ying and E. J. Candes, "Fast geodesics computation with the phase flow method," *Journal of computational physics*, vol. 220, no. 1, pp. 6–18, 2006.
- [9] R. Kimmel and J. A. Sethian, "Computing geodesic paths on manifolds," *Proceedings of the National Academy of Sciences*, vol. 95, no. 15, pp. 8431–8435, 1998.
- [10] Y. Boykov and V. Kolmogorov, "Computing geodesics and minimal surfaces via graph cuts," in *Proc. IEEE International Conference on Computer Vision*, 2003.
- [11] J. T. Betts, *Practical methods for optimal control and estimation using nonlinear programming*. Siam, 2010, vol. 19.
- [12] M. Diehl, H. J. Ferreau, and N. Haverbeke, "Efficient numerical methods for nonlinear MPC and moving horizon estimation," in *Nonlinear Model Predictive Control*. Springer, 2009, pp. 391–417.
- [13] D. A. Benson, G. T. Huntington, T. P. Thorvaldsen, and A. V. Rao, "Direct trajectory optimization and costate estimation via an orthogonal collocation method," *Journal of Guidance, Control, and Dynamics*, vol. 29, no. 6, pp. 1435–1440, 2006.
- [14] G. N. Elnagar and M. A. Kazemi, "Pseudospectral Chebyshev optimal control of constrained nonlinear dynamical systems," *Computational Optimization and Applications*, vol. 11, no. 2, pp. 195–217, 1998.
- [15] F. Fahroo and I. M. Ross, "Direct trajectory optimization by a Chebyshev pseudospectral method," *Journal of Guidance, Control, and Dynamics*, vol. 25, no. 1, pp. 160–166, 2002.
- [16] D. Garg, M. Patterson, W. W. Hager, A. V. Rao, D. A. Benson, and G. T. Huntington, "A unified framework for the numerical solution of optimal control problems using pseudospectral methods," *Automatica*, vol. 46, no. 11, pp. 1843–1851, 2010.
- [17] J. P. Boyd, *Chebyshev and Fourier spectral methods*. Courier Corporation, 2001.
- [18] B. Houska, H. J. Ferreau, and M. Diehl, "ACADO toolkit-An open-source framework for automatic control and dynamic optimization," *Optimal Control Applications and Methods*, vol. 32, no. 3, pp. 298–312, May 2011.
- [19] J. M. Lee, *Riemannian manifolds: an introduction to curvature*. Springer Science & Business Media, 2006, vol. 176.
- [20] W. M. Boothby, *An introduction to differentiable manifolds and Riemannian geometry*. Academic press, 1986, bibtex: boothby1986introduction.
- [21] P. Finsler, "über das vorkommen definiten und semidefiniten formen in scharen quadratischer formen," *Commentarii Math. Helvetici*, vol. 9, no. 1, pp. 188–192, 1936.
- [22] P. A. Parrilo, "Semidefinite programming relaxations for semialgebraic problems," *Mathematical programming*, vol. 96, no. 2, pp. 293–320, 2003.
- [23] L. N. Trefethen, "Is Gauss quadrature better than Clenshaw-Curtis?" *SIAM review*, vol. 50, no. 1, pp. 67–87, 2008.
- [24] J. Nocedal and S. Wright, *Numerical optimization*. Springer Science & Business Media, 2006.
- [25] V. Andrieu and C. Prieur, "Uniting two control lyapunov functions for affine systems," *IEEE Transactions on Automatic Control*, vol. 55, no. 8, pp. 1923–1927, 2010.
- [26] J. Löfberg, "Yalmip: A toolbox for modeling and optimization in matlab," in *Computer Aided Control Systems Design, 2004 IEEE International Symposium on*. IEEE, 2004, pp. 284–289.



